Master Thesis

Synthesis and characterization of three-dimensional ITO nanoelectrodes

Author: **Javier Castillo-Seoane**[a,b].
Tutors: Jorge Gil-Rostra[a], Ana Borras[a], Leidy Marcela Martínez Tejada[b].

[a]Institute of Materials Science of Seville (cicCartuja; CSIC – University of Seville), [b]University of Seville.

Abstract: The aim of this Master Thesis is to show the feasible application of an innovative one-dimensional (1D) soft-template method to the fabrication of supported wide band gap oxides nanotubes (NTs) and nanotrees (NTrees), in our case of Indium Tin Oxide (ITO). Polycrystalline nanotubes were synthesized combining the growth of 1D templates based on single-crystalline organic nanowires (ONWs) of phthalocyanines (H_2Pc) by vapor transport in mild vacuum ("O"PVD) and the conformal deposition of ITO by magnetron sputtering (MS). Experimental conditions for the formation of the ITO nanostructures such as deposition time, deposition pressure and post-annealing treatment were set to control the thickness, alignment and optoelectronic properties of the supported nanotubes. The equivalent deposition in the form of thin film (TF) was also included in the characterization matrix as reference system.

1. Introduction

The use of nanomaterials and industrially scalable and sustainable new synthesis techniques allow the developing of a more efficient technology that can be applied in energy or environmental applications. Nanomaterials present a large variety of applications fields, but it is their implantation in optoelectronic, sensors or energy what has encouraged this work. There are different devices such as light emitting devices (LEDs), solar cells, etc, where we can insert them. These devices have some components which are made by transparent conducting oxides (TCOs). TCOs have taken attention in the last years because their interesting properties such as high transparency with a conductivity comparable with metals [1]. Examples of these oxides are ITO (Indium Tin Oxides), FTO (Fluorine doped Tin Oxide), AZO (Aluminium doped Zin Oxide), etc [2,3].

ITO composition has been selected as reference material in this work because of its extended use in different industries as transparent electrode due to both its high optical transmittance (80% at 500 nm) yet high electrical conductivity (sheet resistance 5 - 10 Ω/□) [4]. It is possible to find in the bibliography different methods of synthesis for ITO thin films such as magnetron sputtering (more extended) [5,6], thermal [7] or e-beam [8] assisted depositions, sol-gel [9], etc, but the interest of this Master Thesis is the synthesis of 1D nanostructures. Previous authors have reported ITO 1D morphologies synthesis as vapor-solid (VS), vapor-liquid-solid (VLS) [10] or template [11,12] methods that imply high temperatures.

The use of 1D nanostructures regarding thin films is encouraged by the possibility of miniaturization, their higher exposed area, their novel properties due to the reduction of scale and the option of synthesize multifunctional devices (heterostructures) [13].

2. Methodology

The methodology that is used in this Master Thesis works in two different ways:

- Synthesis of thin films.
- Synthesis of nanostructured materials (nanotubes and nanotrees).

In this part, we describe the three experimental conditions to synthesize the different nanomaterials in the study.

Firstly, it was deposited **ITO thin films** (**ITO_TF**) on different substrates in two conditions. These thin films were used as a benchmark to compare with the 1D and 3D nanomaterials. The deposition method was magnetron sputtering (RF Ar plasma) at two deposition conditions addressed from now as low pressure ($5 \cdot 10^{-3}$ mbar), LP, and high pressure ($2 \cdot 10^{-2}$ mbar), HP.

Secondly, **ITO nanotubes** (**ITO_NTs**) were formed on the surface of the different substrates. The fabrication method consists on a sequential soft template method of four steps (see Figure 1): i) formation of nucleation centers, ii) growth of supported organic nanowires (ONWs) [14,15], iii) formation of ITO shell and iv) evacuation of the organic core from the 1D hybrid core@shell nanostructures to leave an empty ITO nanotube. We also applied a post-annealing in Ar atmosphere.

As final proof of concept, we extended the soft template methodology towards the formation of **ITO nanotrees** (**ITO_NTrees**) (see Figure 2). The deposition method and the conditions were the same than the ITO_NTs samples but i-iii) steps were applied three times to each substrate. Using this approach, a nanostructured material with a three-dimensional morphology (a main central nanotube with secondary branching nanotubes) is formed as it is presented in the results section.

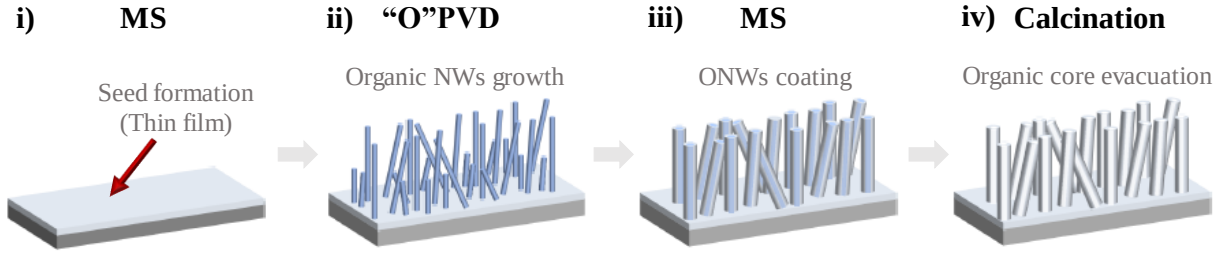

Figure 1. Soft-template method applied to the formation of 1D nanostructures: i) formation of nucleation centers, ii) growth of supported organic nanowires, iii) formation of ITO shell and iv) evacuation of the 1D hybrid core@shell nanostructures.

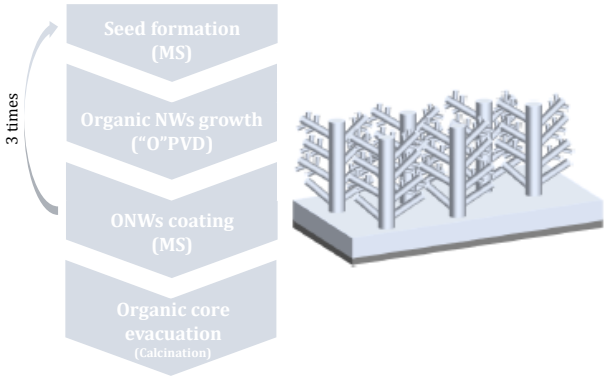

Figure 2. Soft-template method applied to the formation of hierarchical nanostructures: nanotrees/forest.

A detailed characterization including SEM, TEM, XRD, EDXS, XPS, UV-Vis-NIR spectroscopy and advanced electrical measurements were carried out to display the relationship between composition, microstructure, morphology and optoelectronic properties.

3. Results and discussion

Using SEM in Secondary Electrons mode (SE) we analysed the morphology of the samples synthesized.

Figure 3 shows characteristic micrographs of ITO thin films grown at the two different Ar pressures. At first glance, they present the same morphology with triangular and elongated features coexisting on the surface but forming patches or domains. A closed inspection of the planar view images at lower magnification reveals that the size of these domains is larger for the HP conditions. Also, we determined that the deposition rate of HP samples is higher than LP ones.

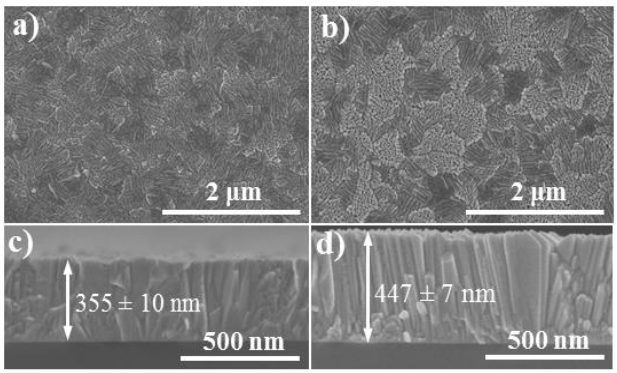

Figure 3. SEM characteristic micrographs in planar view and cross section of: a), c) ITO LP TF and b), d) ITO HP TF.

Figure 4 shows a normal view of the H_2PC ONWs, ITO LP and HP NTs. One of our goals was to reproduce the formation of single-crystalline ONWs on the surface of ITO TF (see Figure 4a). On the other hand, we were able to form polycrystalline NTs coating the organic template using a one reactor configuration (see Figures 4b and 4c).

Table 1 summarizes the statistical SEM analysis for the length and diameter of the 1D nanostructures and their estimated density. Focusing in the density of nanostructures, there is a high decreasing in this magnitude after the ITO shell deposition. It could be associated to a possible sublimation of ONWs during the process due to the low thickness of the protecting coating or because of shadowing effects. Paying attention in the length of the nanostructures, it happens the same with this magnitude. The explanation could be in an equal direction, the sublimation of the organic template causes material losses that elucidate a length decreasing.

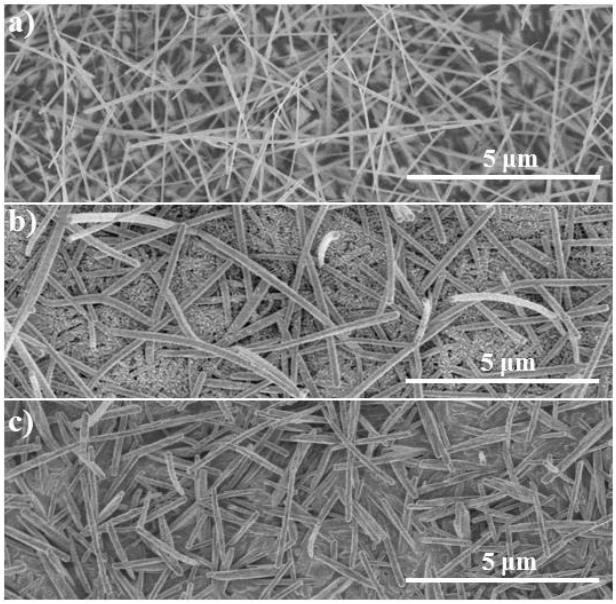

Figure 4. SEM characteristic micrographs in planar view of: a) H_2Pc ONWs grown in ITO LP thin film, b) ITO LP nanotubes and c) ITO_HP nanotubes.

Table 1. Statistical SEM analysis results of ONWs and ITO nanotubes.

Sample/Measure	Diameter, D (µm)	Length, L (µm)	Density (n/µm^2)
H_2Pc_ONWs	0.10 ± 0.03	4.0 ± 1.6	6.5 ± 0.7
ITO_NTs_LP	0.19 ± 0.04	2.2 ± 1.2	2.7 ± 1.0
ITO_NTs_HP	0.22 ± 0.05	2.8 ± 0.9	3.3 ± 0.6

If we observe Figure 5, it is easy to appreciate a different crystalline growth in the two conditions NTs. On one hand, ITO LP NTs show a homogenous morphology along all of their structure with non-defined domains. On the other hand, ITO HP NTs exhibit well-defined morphological domains in good agreement with the previous results about the microstructure of the thin films.

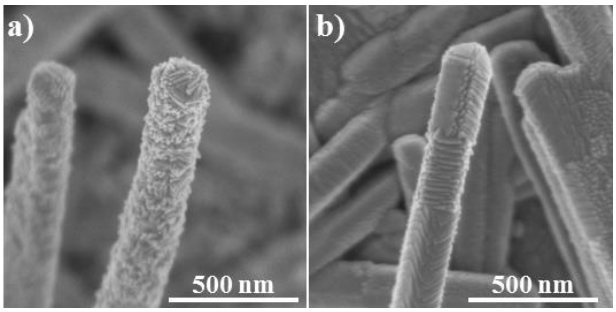

Figure 5. SEM micrographs of the ITO nanotubes samples at high magnification in the two conditions: a) LP and b) HP.

Another purpose of this Master Thesis was the synthesis of 3D hierarchical nanostructures (nanotrees/forest). We applyied the soft-template method in the two same conditions than for the ITO NTs formation but repeating the process (See Section 2). Figure 6 gathers the SEM study of these nanostructures. It is possible to mention that LP nanotrees lead to higher sizes in a less homogeneous distribution (Figure 6 a)), whereas HP samples are well distributed along all the substrate (panel b) and present smaller sizes (panel d).

For the following characterizations, we have selected high-pressure nanotrees due to their greater order, verticality, and homogeneous distribution.

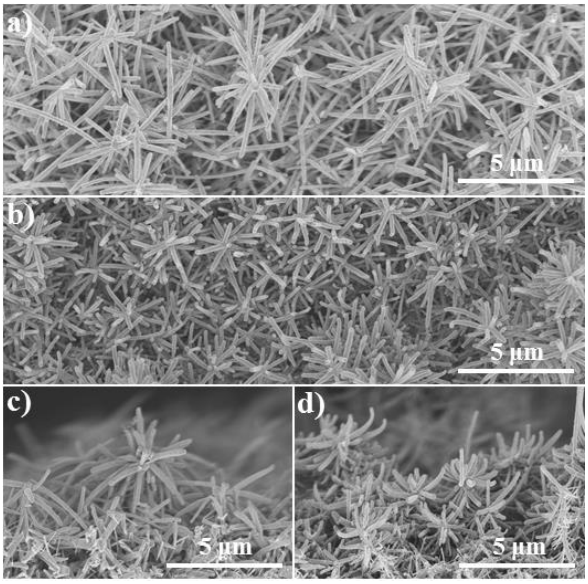

Figure 6. SEM characteristic micrographs in planar view and cross section of: a), c) ITO LP nanotrees and b), d) ITO HP nanotrees.

Hence, we show a part of the TEM study of the nanotubes samples to compare in detail their morphology and crystalline structure. It was possible to observe a lighter area along the axis of the nanotubes corresponding to the conduct or cavity left after the organic template sublimation. Figure 7 shows HRTEM micrographs.

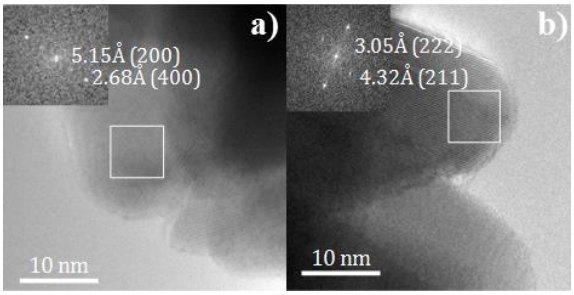

Figure 7. HRTEM micrograph comparative with a digital diffractogram indexed of: a) ITO LP NTs and b) ITO HP NTs.

HRTEM micrographs reveals different crystalline planes that are in concordance with ITO structure. To index them we measure the interplanar length from the digital diffractograms generated.

The XRD study confirms previous results shown. We can observe in Figure 8 a comparison of XRD spectra of the 5 morphologies synthesized where it is possible to appreciate a certain texturization in thin film samples in planes (2 1 1) and (4 0 0) for LP and HP samples respectively.

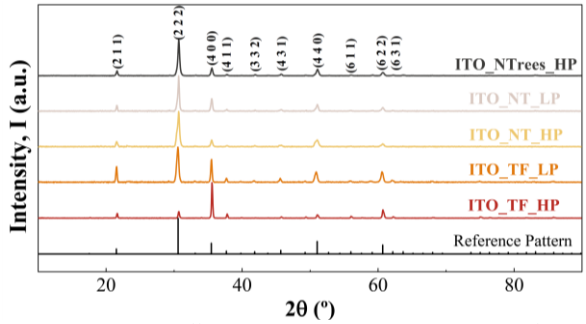

Figure 8. XRD indexed diffractograms comparative among ITO thin film (LP and HP), nanotubes (LP and HP) and nanotrees (HP). Reference pattern taken of PANalytical X'Pert HighScore database: Indium Oxide [Reference code: 00-006-0416].

Regarding the optical characterization, we obtained the tipical beahaviour in the visible range of a transparent material deposited in thin film configuration for our ITO TF samples with a high absorptance in the NIR region that is asociated to their conduction mechanism. Furthermore, we analysed optical response and the effect of the Ar-annealing of the NT and NTrees samples (see Figure 9). In this way, we used an UV-vis-NIR spectrophotometre equiped with an integrator sphere to obtain diffuse components of the ligh spectrum.

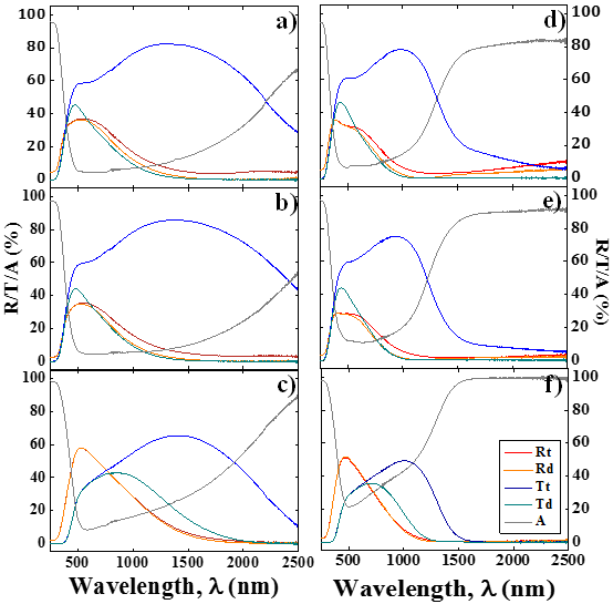

Figure 9. UV-vis-NIR spectra of ITO pre-Ar-annealed (left-side) and post-Ar-annealed (right-side) samples: LP nanotubes (a, d), HP nanotubes (b, e) and HP nanotrees (c, f). It is shown the absorptance (A), the total and diffuse transmittance (T_T, T_D) and reflectance (R_T, R_D).

An in deep discussion of these spectra would require also modelling the optical response of the NTs and NTrees. However, some striking aspects can be addressed. Firstly, it is important to highlight that these nanostructured layers present spectra dominated by scattering effects in the visible range which reduce its transparency, a different behaviour regarding TF ones. Secondly, we can observe a marked effect of the Ar-annealing in the absorptance (grey line). Our hypothesis is that the organic core remove in air could oxidise completely the ITO, losing the O vacancies responsible of the conduction mechanism [3] and the Ar-annealing could reduce the ITO again. All mentioned can be observe in the absorption in the NIR range of the spectra.

Figure 10, 11 and Table 2 summarize the results regarding the electrical characterization of the samples. The idea was to elucidate both electrical resistances, the corresponding to the layer of NTs and NTrees supported on the ITO decorated substrates (Figure 10 a)) and the corresponding to individual nanotubes (Figure 10 b)).

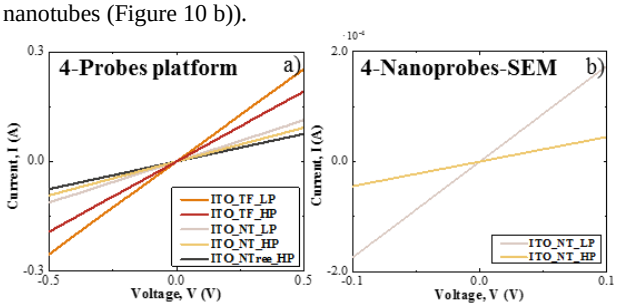

Figure 10. a) I-V curve comparative among ITO thin film (LP and HP), nanotubes (LP and HP) and nanotrees (HP) macroscopic measurements and b) I-V curve comparative between ITO nanotubes (LP and HP) nanoscopic measurements.

Figure 10 a) show the I-V curves obtained for the five type of samples, including the LP and HP thin films. All these curves present a linear dependence between the current (I) and the voltage (V) in the studied range (-0.5 and 0.5 V) with different slopes corresponding to the variations in resistance (R) of the samples.

The accurate elucidation of the NTs electrical conductivity requires of the characterization in a single-wire approach, i.e. contacting the NTs as individual items. Such advanced characterization has been for the first time carried out systematically by the Nanotechnology on Surfaces group in the context of this Master Thesis. I-V curves in Figure 10 b) are representative from both type of NTs and the values in Table 2 were calculated after analysis of three different NTs from each condition and five I-V curves. In good agreement with the previous results, the ITO_NTs resistivity for the HP conditions is higher than for the LP, both of them in a very low range, and in the case of LP conditions, comparable to the reported for single crystalline ITO NWs fabricated by VLS ($2.4 \cdot 10^{-6}$ Ω·m) [10].

Table 2. 4-point probe conductivity measures results (nanoscale).

Sample/Measure	Resistivity, ρ (Ω·m)
ITO_NTs_LP	$(3.5 \pm 0.9) \cdot 10^{-6}$
ITO_NTs_HP	$(1.5 \pm 0.7) \cdot 10^{-5}$

Figure 11 shows SEM images taken during the electrical characterization in nanoscale. In these, we can observe one nanotube with four Pt electrical contacts and the 4 nanoprobes on them.

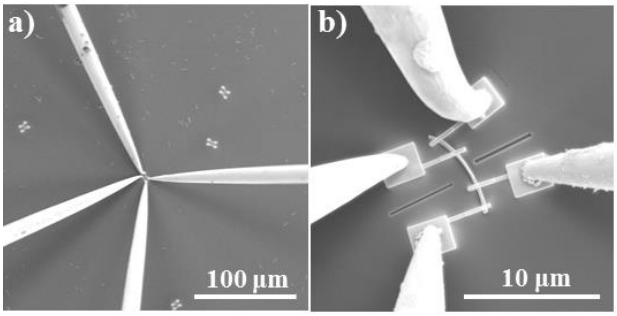

Figure 11. Representative SEM images showing the electrical characterization of an ITO nanotube by four-nanoprobes assisted by a micromanipulator platform installed in a SEM chamber.

4. Conclusions

We have elucidated the potentiality of the "one-reactor" configuration in the synthesis by a soft-template technique, proving that an "organic" PVD and a magnetron sputtering deposition can be combined to fabricate transparent metal oxides nanotubes, core@shell, and hierarchical nanostructures.

We have synthetized ITO thin films in two pressure conditions (LP and HP) with transparency in the visible range above the 80% and low resistivity ($\rho < 5 \cdot 10^{-6}$ Ω·m), these values are strongly competitive with previous references applying RF and DC sputtering [5,6].

We have synthesized crystalline ITO nanotubes with crystal sizes lower than 100 nm, homogeneously distributed along the nanotube cavity. The ITO NTs present three-dimensional shells formed by polycrystalline ITO. The morphology of the LP_NTs is more homogeneous along the NT length and consist of triangular shape grains. HP_NTs show a microstructure characterized by the formation of domains of crystals, sharing shape and orientation.

XPS, XRD and UV-VIS-NIR results are in good agreement with the formation of highly conductive nanostructures with high absorptance in the NIR. Optical bandgaps for the HP_TF and 1D/3D nanostructures are smaller than for the LP TF and bulk. Conductivity of the 1D and 3D nanostructures is smaller than the thin films counterparts ($\rho_{LP\_TF} < \rho_{HP\_TF} < \rho_{LP\_NT} < \rho_{HP\_NT}$). It is remarkable that our polycrystalline ITO NTs have comparable conductivities to monocrystalline ITO NWs measuring by equivalent methods. All the estimated values for sheet resistance and resistivities indicate that these nanoelectrodes comply with the requirements for their implementation in solar cells and photoelectrochemical processes.

We have demonstrated that the method is extensible to the formation of ITO Ntrees. HP conditions provide highly ordered and homogeneous 3D architectures.

5. References

[1] Yu, X., Marks, T., & Facchetti, A. (2016). Metal oxides for optoelectronic applications. Nature Materials, 15(4), 383-396. doi: 10.1038/nmat4599

[2] Morales-Masis, M., De Wolf, S., Woods-Robinson, R., Ager, J., & Ballif, C. (2017). Transparent Electrodes for Efficient Optoelectronics. Advanced Electronic Materials, 3(5), 1600529. doi: 10.1002/aelm.201600529

[3] Ma, Z., Li, Z., Liu, K., Ye, C., & Sorger, V. (2015). Indium-Tin-Oxide for High-performance Electro-optic Modulation. Nanophotonics, 4(1). doi: 10.1515/nanoph-2015-0006

[4] Liu, H., Avrutin, V., Izyumskaya, N., Özgür, Ü., & Morkoç, H. (2010). Transparent conducting oxides for electrode applications in light emitting and absorbing devices. Superlattices And Microstructures, 48(5), 458-484. doi: 10.1016/j.spmi.2010.08.011

[5] Cui, H., Teixeira, V., Meng, L., Martins, R., & Fortunato, E. (2008). Influence of oxygen/argon pressure ratio on the morphology, optical and electrical properties of ITO thin films deposited at room temperature. Vacuum, 82(12), 1507-1511. doi: 10.1016/j.vacuum.2008.03.061

[6] Yang, C., Lee, S., Chen, S., & Lin, T. (2006). The effect of annealing treatment on microstructure and properties of indium tin oxides films. Materials Science and Engineering: B, 129(1-3), 154-160. doi: 10.1016/j.mseb.2006.01.012

[7] Granqvist, C., & Hultåker, A. (2002). Transparent and conducting ITO films: new developments and applications. Thin Solid Films, 411(1), 1-5. doi: 10.1016/s0040-6090(02)00163-3

[8] Parra-Barranco, J., García-García, F., Rico, V., Borrás, A., López-Santos, C., & Frutos, F. et al. (2015). Anisotropic In-Plane Conductivity and Dichroic Gold Plasmon Resonance in Plasma-Assisted ITO Thin Films e-Beam-Evaporated at Oblique Angles. ACS Applied Materials & Interfaces, 7(20), 10993-11001. doi: 10.1021/acsami.5b02197

[9] Su, C., Sheu, T., Chang, Y., Wan, M., Feng, M., & Hung, W. (2005). Preparation of ITO Thin Films by Sol-Gel Process and Their Characterizations. Synthetic Metals, 153(1-3), 9-12. doi: 10.1016/j.synthmet.2005.07.219

[10] Gao, J., Chen, R., Li, D., Jiang, L., Ye, J., & Ma, X. et al. (2011). UV light emitting transparent conducting tin-doped indium oxide (ITO) nanowires. Nanotechnology, 22(19), 195706. doi: 10.1088/0957-4484/22/19/195706

[11] Sumboja, A., Wang, X., Yan, J., & Lee, P. (2012). Nanoarchitectured current collector for high rate capability of polyaniline-based supercapacitor electrode. Electrochimica Acta, 65, 190-195. doi: 10.1016/j.electacta.2012.01.046

[12] Li, Q., Wang, S., Zhang, M., Feng, L., Su, X., & Ding, W. et al. (2018). ITO nanowire networks coating on μ-hole arrayed substrate as super-broadband antireflection layer. Solar Energy, 173, 590-596. doi: 10.1016/j.solener.2018.08.005

[13] Filipin A. N. (2015). Development of Supported 1D Nanomaterials by Vacuum and Plasma Technologies: From Sensors to Nanogenerators. (PhD thesis). University of Seville – CSIC.

[14] Borras, A., Aguirre, M., Groening, O., Lopez-Cartes, C., & Groening, P. (2008). Synthesis of Supported Single-Crystalline Organic Nanowires by Physical Vapor Deposition. Chemistry Of Materials, 20(24), 7371-7373. doi: 10.1021/cm802172p

[15] Borras, A., Gröning, O., Aguirre, M., Gramm, F., & Gröning, P. (2010). One-Step Dry Method for the Synthesis of Supported Single-Crystalline Organic Nanowires Formed by π-Conjugated Molecules. Langmuir, 26(8), 5763-5771. doi: 10.1021/la1003758